Structural and Binding Properties of the Stilbenedisulfonate Sites on Erythrocyte Band 3: An Electron Paramagnetic Resonance Study Using Spin-Labeled Stilbenedisulfonates†

Walter E. Wojcicki and Albert H. Beth*

Department of Molecular Physiology and Biophysics, Vanderbilt University, Nashville, Tennessee 37232-0615

Received May 20, 1993®

ABSTRACT: Two new spin-label derivatives of 4,4′-diaminodihydrostilbene-2,2′-disulfonate (H_2-DADS) have been chemically synthesized and employed in electron paramagnetic resonance (EPR) studies of binding to the anion exchange protein (band 3) in intact human erythrocytes. Equilibrium binding studies with the 4-monoacyl-spin-label derivative (mono-SL-H_2-DADS) indicated an effective dissociation constant of 11 μM and substantial negative cooperativity in isotonic citrate buffer, pH 7.4, at 20 °C. The 4,4′-diacyl-spin-label derivative (di-SL-H_2-DADS) bound with an effective dissociation constant of 54 μM and no detectable cooperativity under the same binding conditions. The findings of substantial negative cooperativity in binding of the less bulky mono-SL-H_2-DADS and no cooperativity for di-SL-H_2-DADS suggest the presence of an allosteric coupling between the stilbenedisulfonate sites on adjacent band 3 monomers rather than steric interactions. There were approximately 1×10^6 binding sites per erythrocyte for both the mono- and di-SL-H_2-DADS derivatives, and the binding of each was blocked by pretreatment of intact cells with 4,4′-diisothiocyanostilbene-2,2′-disulfonate (DIDS), a highly specific covalent inhibitor of anion exchange. EPR spectra collected over a wide range of concentrations of mono-SL-H_2-DADS indicated that binding resulted in immobilization of the probe and that, even upon near saturation of available binding sites, there were no detectable dipole–dipole interactions between bound probes. EPR spectra collected using di-SL-H_2-DADS revealed the presence of intramolecular dipole–dipole interactions between spin-label moieties on opposite ends of this biradical probe, but no intermolecular dipole–dipole interactions between separate bound probes. These data indicate that di-SL-H_2-DADS binds to the stilbenedisulfonate binding site on band 3 in a bent conformation and further suggest that the termini of these binding sites on adjacent monomers are greater than 20 Å apart.

The anion exchange protein (band 3) in human erythrocytes has been studied extensively over the past two decades with regard to its role in exchange of Cl^- and HCO_3^- across the membrane [for reviews, see Knauf (1979), Passow (1986), Jay and Cantley (1986), and Jennings (1984, 1989)]. Early studies demonstrated that both covalent and noncovalent binding derivatives of stilbenedisulfonate were highly specific for band 3 in intact cells and that these probes were useful in identifying band 3 as the anion exchanger in erythrocytes (Cabantchik & Rothstein, 1972, 1974) and in working out details of the anion exchange mechanism (Barzilay & Cabantchik, 1979). However, the oligomeric state of association of band 3 in native erythrocyte membranes and the spatial distribution of the stilbenedisulfonate binding sites have remained largely unresolved. Steck (1972) showed that band 3 can be covalently cross-linked in erythrocyte ghost membranes by mild oxidation to form dimers. Staros and co-workers (1982, 1983) used the membrane-impermeant protein cross-linking reagent bis(sulfo-*N*-succinimidyl) suberate (BS^3)[1] to show dimer formation in intact erythrocytes. Higher order association states have been reported (Salhany & Sloan, 1988), which are generally attributed to tetramers formed by the dimerization of dimers (Staros & Kakkad, 1983). Freeze-fracture studies of erythrocyte membranes have supported the evidence from biochemical and biophysical studies that show that self-association of membrane-bound band 3 monomers occurs *in situ*. Weinstein et al. (1980a) surveyed electron micrograph data from several laboratories and determined the number of intramembranous particles to be in the range of 3.6×10^5 to 4.5×10^5 particles per cell. There is evidence that these band 3 containing intramembranous particles are heterogeneous in size, which may mean that some particles contain dimers of band 3 and some contain tetramers (Margaritis et al., 1977, Weinstein et al., 1980b). The number of copies of the band 3 monomer per cell has been shown to be $\sim 1 \times 10^6$. Thus, EM data support the hypothesis that band 3 is dimeric, tetrameric, or some combination of the two in the membrane [reviewed in Jennings (1984)]. The dimeric association between subunits is very stable in erythrocyte membranes (Nigg & Cherry, 1979, Anjaneyulu et al., 1988), and in detergent solutions (Casey & Reithmeier, 1991). Despite the uncertainty in the oligomeric state of band 3 *in situ* (i.e., dimer versus tetramer), there is reasonable agreement that the dimer of band 3 is the fundamental species (Staros & Kakkad, 1983), and that this

† This work was supported by Grants HL34737, RR04075, and T32GM07347 from the National Institutes of Health.

* To whom correspondence should be addressed at the Department of Molecular Physiology and Biophysics, 727 Light Hall, Vanderbilt University, Nashville, TN 37232-0615.

® Abstract published in *Advance ACS Abstracts*, August 15, 1993.

[1] Abbreviations: BIDS, 4-benzamido-4′-isothiocyanostilbene-2,2′-disulfonate; BSSDP, bis(sulfo-*N*-succinimidyl) doxyl-2-spiro-4′-pimelate; BS^3, bis(sulfo-*N*-succinimidyl) suberate; [^{15}N]CAT-1, 4-(trimethylammonium)-2,2,6,6-tetramethylpiperidine-d_{17}-*1*-^{15}*N*-1-oxyl, iodide; DADS, 4,4′-diaminostilbene-2,2′-disulfonate; DIDS, 4,4′-diisothiocyanostilbene-2,2′-disulfonate; EPR, electron paramagnetic resonance; H_2-DADS, 4,4′-diaminodihydrostilbene-2,2′-disulfonate; $H_2(NBD)_2DS$, 4,4′-bis(4-nitro-2,1,3-benzoxadiazolyl)dihydrostilbene-2,2′-disulfonate; V_1, first-harmonic in-phase absorption EPR signal.

0006-2960/93/0432-9454$04.00/0

species is capable of binding stilbenedisulfonates with high affinity (Boodhoo & Reithmeier, 1984).

Stilbenedisulfonates, which inhibit erythrocyte anion exchange, have been extensively used to study band 3 structure and function. These ligands bind with high affinity and high specificity for the outward-facing anion exchange site of band 3 in intact erythrocytes and complete with transportable anions including chloride and sulfate. Although many stilbenedisulfonates bind with no detectable cooperativity, a few of the derivatives examined have shown evidence of negative cooperativity which is sensitive to the ionic strength and composition of the buffer (Macara & Cantley, 1981; Verkman et al., 1983; Dix et al., 1986).

Although the influence of the state of association of band 3 on anion transport is not known, dimerization appears to be essential for formation of the stilbenedisulfonate binding site. Boodhoo and Reithmeier (1984) showed that solubilized monomeric band 3 could not bind stilbenedisulfonates, but dimeric band 3 could bind them with high affinity. These data suggest two possible structural models for functional band 3. In the first model, dimerization forms a common anion transport pore or pathway between monomers. In the alternative model, dimerization forms two separate pathways, either one in each monomer subunit, or, alternatively, at two distinct locations at the interface between monomers. The latter model, two separate pathways, is supported by stoichiometry of anion exchange inhibition by stilbenedisulfonates where one inhibitor per monomer is required to approach full inhibition (Ship et al., 1977; Lepke et al., 1976).

Macara and Cantley (1981) have reported the results of a study to measure the distance between neighboring stilbenedisulfonate binding sites on adjacent monomers using fluorescence resonance energy transfer. They reported the donor–acceptor distance between two stilbenedisulfonate fluorophores to be 28–52 Å. This wide range was primarily attributed to uncertainties in the orientation of the transition dipole moments of the immobile bound probes BIDS and $H_2(NBD)_2DS$, the donor–acceptor pair. In addition, they reported that occupation of the anion exchange binding site on one subunit of a band 3 dimer by BIDS results in a decrease in the affinity of the site on the adjacent subunit for the binding of $H_2(NBD)_2$-DS. This decrease in binding affinity might be explained by steric hindrance if neighboring binding sites are close. Macara and Cantley (1981) could not rule out that these large fluorophore molecules might be very close to one another when bound to band 3 and could possibly be occupying overlapping binding sites; i.e., the minimum donor–acceptor separation of 28 Å is similar to the distance between the centers of BIDS and $H_2(NBD)_2DS$ when they are laid end to end.

EPR spectroscopy, which is sensitive to the electron–electron dipolar interactions between neighboring unpaired electrons, offers a means by which the separation geometry between two immobile nitroxide spin-label reporter molecules can be determined. Dipolar interactions are highly dependent on the distance and angles between neighboring nitroxide moieties. Anjaneyulu et al. (1988) employed the spin-labeled cross-linker bis(sulfo-*N*-succinimidyl) doxyl-2-spiro-4′-pimelate (BSSDP), an affinity label for the exofacial domain of band 3, to demonstrate a >16-Å separation between probe reaction sites on adjacent monomers. However, even though BSSDP blocks covalent reaction of 4,4′-diisothiocyanostilbene-2,2′-disulfonate (DIDS) with band 3, its position relative to the stilbenedisulfonate binding site has not been firmly established. To facilitate study of the stilbenedisulfonate site of band 3, two new EPR spin-label probes containing one or two pyrroline nitroxide groups attached to 4,4′-diaminodihydrostilbene-2,2′-disulfonate (H_2-DADS) have been synthesized. Although these probes, like the fluorophores used by Macara and Cantley (1981), are large molecules, the spin-labeled H_2-DADS derivatives provide quantitative information on the spatial separation and arrangement of specific loci (i.e., the localized nitroxide moieties) when bound to the band 3 binding site. The EPR spectra obtained using these new probes provide evidence that the termini of stilbenedisulfonate binding sites on adjacent subunits of the band 3 dimer are more than 20 Å apart. In addition, because of the intramolecular dipolar and spin–spin exchange interactions possible with a disubstituted nitroxide spin-label, the diradical probe provides information on the conformation of the probe when bound to the stilbenedisulfonate binding site of band 3, thus providing an indication of the expanse of the binding site. Portions of this work have been published as an abstract (Wojcicki et al., 1992).

EXPERIMENTAL PROCEDURES

General Procedures. Human erythrocytes were obtained from the freshly drawn venous blood of volunteer subjects. Blood was drawn into heparinized Vacutainer tubes and combined with 5 volumes of cold (0–4 °C) isotonic buffer (113 mM sodium citrate, pH 7.4) and washed free of other formed elements, serum proteins, and plasma by three suspension and centrifugation cycles. Packed erythrocytes from the final wash were subsequently used for experimentation. A 1-mL aliquot of packed cells was added 1:1 (v/v) to isotonic buffer and analyzed on a Coulter Counter to determine the density of the packed cells. Coulter Counter data were used to account for variability in the cell packing density.

Preparation of Na_2-H_2-DADS. The starting material, 4,4′-diaminostilbene-2,2′-disulfonate (DADS), was obtained from Eastman Kodak (technical grade) as the diacid. To obtain the reduced dihydro form (H_2-DADS), 50 g of DADS was added to 100 mL of deionized water and the pH adjusted to 7.0 with NaOH, resulting in a bright yellow solution which was vacuum filtered to remove traces of insoluble material. The filtered solution was transferred to a hydrogenation bottle, and 1 g of palladium on activated carbon catalyst (Aldrich, 10% palladium) was added. Hydrogenation was carried out overnight on a Parr hydrogenator under 50 psi of hydrogen gas pressure. The resulting suspension was vacuum filtered to remove the palladium catalyst and the product precipitated by adjusting the pH of the resulting colorless solution to 3.0 with HCl. The dense white precipitate, recovered by vacuum filtration followed by washing with cold distilled water, was dried over P_2O_5 in a vacuum desiccator.

A 10-g sample of the H_2-DADS was converted to the disodium salt by addition to 50 mL of deionized water, titration to pH 7.5 with NaOH, and addition of 1.5 volumes of ethanol. The sample was left overnight at 4 °C, during which time a dense layer of translucent crystals formed. The crystals were separated by vacuum filtration, washed with a small volume of cold ethanol, and stored over P_2O_5 in a vacuum desiccator. Thin-layer chromatography of the isolated crystals showed a single spot under 254-nm illumination ($R_f \approx 0.4$) on fluorescent silica gel G plates (50:50:5 methanol/chloroform/ammonium hydroxide).

Preparation of Mono- and Di-SL-H_2-DADS. A 300-mg sample of Na_2-H_2-DADS (0.72 mmol) was weighed and transferred to a 5-mL round-bottom flask. The flask was heated to 180 °C for 1 h in an oil bath with strong vacuum

for sample drying. After cooling to room temperature, 270 mg (0.72 mmol) of the anhydride of 2,2,5,5-tetramethyl-3-pyrroline-d_{13}-*1*-^{15}N-1-oxyl-3-carboxylic acid, prepared from 2,2,5,5-tetramethyl-3-pyrroline-d_{13}-*1*-^{15}N-1-oxyl-3-carboxylic acid (Merck) exactly as described by Rozantsev (1970), was added and the reactants were dissolved in 2 mL of dry *N,N*-dimethylformamide (DMF) (dried over 3-Å molecular sieves). The flask was purged with argon, a stirring bar was added, and the flask was sealed with a $CaCl_2$ drying tube. With stirring, the reaction was heated to 70 °C with a heating mantle for 2 h and then allowed to cool to room temperature. DMF was removed under vacuum on a rotary evaporator, yielding an amorphous yellow solid. Normal isotope [^{14}N,^{1}H] derivatives were synthesized using exactly the same procedures, except normal isotope 2,2,5,5-tetramethyl-3-pyrroline-1-oxyl-3-carboxylic acid (Kodak) was employed in place of the [^{15}N,$^{2}H_{13}$]acid.

Purification of Mono- and Di-SL-H_2-DADS. The solid material from the previously described synthesis was dissolved in 1 mL of methanol and applied in a uniform band to a 20 × 20 cm preparative silica gel G plate (1000-μm stationary phase; Fischer) with fluorescent indicator. The plate was developed using a mobile phase of methanol/chloroform/NH_4OH (50:50:5). Following drying of the plate, three dense bands were observed by 254-nm illumination, the lower one comigrating with unreacted Na_2-H_2-DADS applied in a single spot to the plate for identification of bands. The two more mobile bands were separately scraped from the plate and the compounds present solubilized from the silica particles by addition of 3 volumes of methanol. Silica particles were removed from each suspension by vacuum filtration through nylon filters (0.45 μm; Alltech), and the methanol was removed by rotary evaporation. The residue from each of the bands was dissolved in 2 mL of deionized water and applied to separate Dowex 50W-X8 cation exchange columns (Na salt form) poured to 5-cm height in Pasteur pipets. The eluent from each column was collected in a lyophilization flask and lyophilized to dryness, yielding fluffy yellow solids. Analytical TLC of the isolated solids showed that the intermediate band yielded a single dense spot ($R_f \approx 0.6$) and the upper band a single dense spot ($R_f \approx 0.8$) when visualized by 254-nm illumination. A sample of the intermediate band prepared by dissolving the solid material in 113 mM citrate buffer, pH 7.4, gave a strong EPR signal characteristic of a rapidly tumbling nitroxide. A sample of the upper band, prepared in the same way, also gave a strong EPR signal characteristic of weak spin–spin coupling of a rapidly tumbling nitroxide (see Results). Mass spectral analyses were carried out to confirm the identity of the two bands. Using FB^+ ionization techniques, the intermediate band gave a molecular ion (MH^+) at 583 mass units corresponding to the disodium salt of mono-SL-H_2-DADS, while the upper band gave a molecular ion (MH^+) of 749 mass units corresponding to the disodium salt of di-SL-H_2-DADS. The yield of mono-SL-H_2-DADS was 127 mg (0.22 mmol), and that of the di-SL-H_2-DADS was 153 mg (0.20 mmol) after purification.

EPR Measurements. X-band (9.8 GHz) EPR spectra were recorded on a Bruker ESP-300 spectrometer equipped with an ER-4103 TM_{110} cavity. Samples containing packed erythrocytes were loaded into a WG-813 (Wilmad Glass Co.) aqueous flat cell; cell-free aqueous samples were loaded into 50-μL disposable borosilicate glass tubes (Corning). The temperature was controlled with an ER-111VT variable-temperature unit by blowing nitrogen gas into the cavity. V_1 EPR spectra were recorded at 100-kHz field modulation using a microwave observer power of 10 mW (flat cell) or 2 mW (tubes). The modulation amplitude was 1.0 G (peak-to-peak) for the recording of [^{14}N]spin-label spectra and 0.5 G for recording of the narrower ^{15}N lines. Signal-averaged EPR spectra were recorded using the ESP-300 digital data system.

Preparation of Samples To Obtain Bound Spectra for Quantitating Binding at Low Stoichiometries. Packed erythrocytes from the final wash (General Procedures, above) were labeled with mono- or di-SL-H_2-DADS by adding a 0.06-mL aliquot of spin-labeled H_2-DADS dissolved in isotonic citrate buffer to a 0.44-mL aliquot of packed cells to obtain a 0.50-mL sample of the desired concentration. Each sample was mildly vortexed to promote mixing and allowed to equilibrate at room temperature for a few minutes. The samples were loaded into the flat cell and positioned in the temperature-controlled spectrometer cavity. Unbound-only subtraction spectra were obtained by pretreating cell suspensions prior to labeling with the potent anion exchange inhibitor DIDS to block the reversible binding of spin-labeled H_2-DADS to band 3. Pretreatment of packed red blood cells was accomplished by mixing an appropriate aliquot of a freshly prepared 1.0 mM stock solution of DIDS with the erythrocyte suspension and incubating the mixture for 1 h at room temperature to allow sufficient time for all binding sites to be covalently blocked by DIDS (Cobb et al., 1990). The final average DIDS concentration was 100 μM, which represents an approximately 5-fold molar excess over band 3 monomers. Unbound-only subtraction spectra were recorded using similar spin-label concentrations to avoid any concentration dependencies in the unbound line shapes. The residual bound spectra were numerically integrated to determine the concentration of bound probe. These data were employed to quantitate binding at low stoichiometries.

Preparation of Aqueous Cell-Free Samples To Obtain Binding Curve Data near Saturation. Packed erythrocytes were labeled with [^{14}N]mono- or [^{14}N]di-SL-H_2-DADS by combining a 0.30-mL aliquot of cells with a 0.30-mL isotonic citrate buffer solution containing [^{14}N]spin-labeled H_2-DADS and [^{15}N]CAT-1, a membrane-impermeant cationic spin-label added to precisely measure the volume of extracellular water in the sample. Samples were mixed by mild vortexing in 1.7-mL microcentrifuge tubes (Intermountain Scientific Corp.) and then centrifuged at low speed (1500–2000 rpm) for 15 min to pack the cells. The supernatant was then drawn up by capillary action into 50-μL disposable tubes and placed in the spectrometer. Resulting spectra (not shown) contain five readily distinguishable sharp lines: three lines from the [^{14}N]-SL-H_2-DADS and two lines from the [^{15}N]CAT-1. The concentrations of each of the spin-label compounds are then determined by either measuring the peak heights or integrating the lines and comparing with a standard curve obtained using buffer only. The dilution of [^{15}N]CAT-1 was used to precisely measure the extracellular aqueous volume. This volume times the concentration of [^{14}N]SL-H_2-DADS in solution gives the number of unbound moles of the spin-label. Because the total number of moles of the spin-label added to the sample must be conserved, the difference between the total and unbound moles is the amount of the spin-label bound to band 3.

Analysis of Bound EPR Spectra. Each V_1 EPR spectrum obtained from spin-label-containing erythrocyte suspensions is a composite which consists of components from both bound and unbound spectra. The bound spectrum was determined from the composite spectrum by numerical subtraction of an unbound-only spectrum, scaled to the same amplitude. The bound spectra obtained using this subtraction technique were

subsequently analyzed by computer methods which use mathematical simulations of rigid limit EPR spectra, and which include electron–electron dipolar and exchange interactions.

Elements of the nitrogen hyperfine (**A**) and electron-Zeeman (**g**) tensors, as well as the line width (T_2), which are required as input for the computer simulations, were determined by the best fit to the experimental ^{15}N monosubstituted bound spectrum as described by Hustedt et al. (1992).

Electron–electron dipolar interactions between neighboring nitroxide groups will give rise to complex alterations in the EPR line shape. Spectra can be analyzed to determine the degree of dipole–dipole interaction, which is highly dependent upon the distance and geometry between the nitroxide moieties. The distance and geometry parameters, which define the spatial relationships between interacting nitroxides, were determined by the method of Beth et al. (1984), who used the computer program MENO developed by Eaton et al. (1983) to simulate the dipolar spectra of spin-labeled NAD^+ bound to the enzyme glyceraldehyde-3-phosphate dehydrogenase. MENO mathematically simulates dipolar spectra by applying a spin Hamiltonian of the form

$$\mathcal{H} = \mathbf{H}\cdot\mathbf{g}_1\cdot\mathbf{S}_1 + \mathbf{I}_1\cdot\mathbf{A}_1\cdot\mathbf{S}_1 + \mathbf{H}\cdot\mathbf{g}_2\cdot\mathbf{S}_2 + \mathbf{I}_2\cdot\mathbf{A}_2\cdot\mathbf{S}_2 + \mathbf{S}_1\cdot\mathbf{D}\cdot\mathbf{S}_2 + J\mathbf{S}_1\cdot\mathbf{S}_2$$

where $\mathbf{H}$ = external magnetic field, $\mathbf{I}_1$ and $\mathbf{I}_2$ = nuclear spin operators for the two nitroxide nitrogen nuclei, $\mathbf{S}_1$ and $\mathbf{S}_2$ = spin operators for the two interacting electrons, $\mathbf{g}_1$ and $\mathbf{g}_2$ = electron-Zeeman tensors, $\mathbf{A}_1$ and $\mathbf{A}_2$ = nitrogen hyperfine tensors, $\mathbf{D}$ = dipolar coupling tensor, and J = isotropic exchange term.

After the elements of the **A** and **g** tensors, as well as the line width, were determined by fitting the bound [^{15}N]mono-SL-H_2-DADS spectrum, the distance and geometry parameters associated with the intramolecular dipolar interactions observed in the [^{15}N]-SL-H_2-DADS bound spectra were determined. For these calculations, it was assumed that the two nitroxides were equivalent, *i.e.*, the **A** and **g** tensor values and line width are the same for both nitroxides. To determine the dipolar coupling parameters, the **A** and **g** tensor values, along with the line width, were held fixed and the best-fit values of the magnitude of the interelectron vector, $|\mathbf{R}_{1,2}|$, and the angles ξ, η, A_1, A_2, and A_3 were found [where ξ and η are the polar angles for $\mathbf{R}_{1,2}$ in the reference frame of spin-label 1, and A_1, A_2, and A_3 are the polar angles relating spin-label 2 to spin-label 1 (Eaton et al., 1983)].

All best-fit EPR spectra from di-SL-H_2-DADS were determined by finding the global minimum of the multidimensional error surface which was generated by χ^2 comparison of computed spectra with the experimental spectrum to be fitted. The simple, but robust, downhill-simplex method of function minimization was used to locate minima on the error surface [source code was adapted from Press et al. (1989)]. The global minimum was assumed to be the minimum with the lowest residual error. All mathematical simulations were coded in the C programming language. They were compiled and run under Stardent UNIX Release 2.2 on an Ardent Titan computer.

Molecular Modeling. A model of the disubstituted spin-labeled H_2-DADS compound was constructed using the Insight II molecular modeling program. Molecular dynamics simulations were run using the program Discover. A shell of 113 water molecules was included in the molecular dynamics simulations to help shield the large intramolecular electrostatic repulsion forces between the sulfonate groups. Insight II and Discover are software packages available from Biosym Technologies, San Diego, CA. They were run under IRIX System V.3 on a Silicon Graphics workstation.

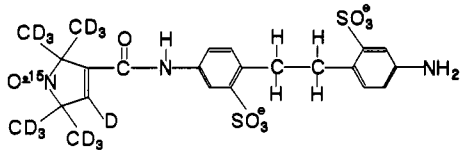

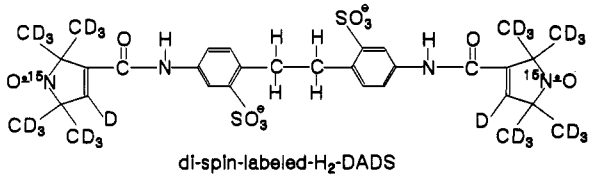

FIGURE 1: Chemical structures of the two new spin-label derivatives of the stilbenedisulfonate compound H_2-DADS used in this study.

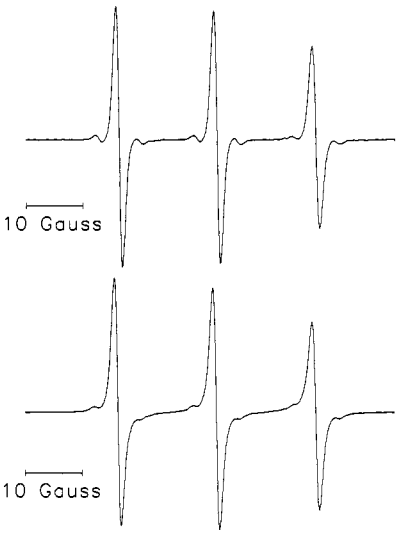

FIGURE 2: X-band (9.8 GHz) spectra of 100 μM aqueous solutions of [^{14}N]mono-SL-H_2-DADS (upper panel) and [^{14}N]di-SL-H_2-DADS (lower panel). The sample temperature was 20 °C, and the scan range was 60 G.

RESULTS

EPR Spectra from Dilute Aqueous Solutions of Mono- and Di-Spin-Labeled H_2-DADS. Figure 1 shows the chemical structures of the two SL-H_2-DADS derivatives which were synthesized and employed in these studies. Figure 2 shows X-band (9.8 GHz) EPR spectra from 100 μM samples of each of the two [^{14}N]spin-label compounds dissolved in isotonic buffer. The spin-label molecules undergo rapid rotational motion in an isotropic medium and have their spectral anisotropy completely averaged, thus giving rise to the three-line EPR spectrum typified by the [^{14}N]mono-SL-H_2-DADS spectrum shown in the upper panel of Figure 2. The [^{14}N]-di-SL-H_2-DADS spectrum of Figure 2 (lower panel) is clearly different from the corresponding mono-spin-label spectrum. The distorted line shape is suggestive of an intramolecular exchange interaction between the two nitroxide groups of the di-spin-label compound.

In general, EPR line widths are affected by a variety of spin relaxation processes, but for the monoradical spin-label, the dominant process is associated with anisotropic interactions coupled to the molecular rotation. Because the rate of molecular reorientation is strongly influenced by the viscosity

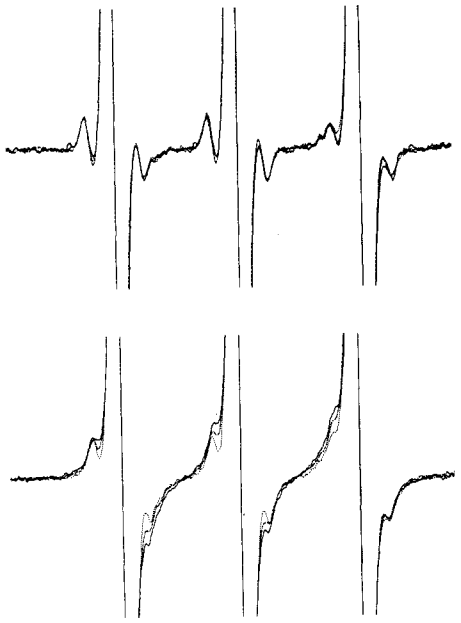

FIGURE 3: EPR spectra of 100 μM aqueous samples of [^{14}N]mono-SL-H_2-DADS (upper panel) and [^{14}N]di-SL-H_2-DADS (lower panel) recorded at 2 °C (···), 22 °C (- - -), and 40 °C (—).

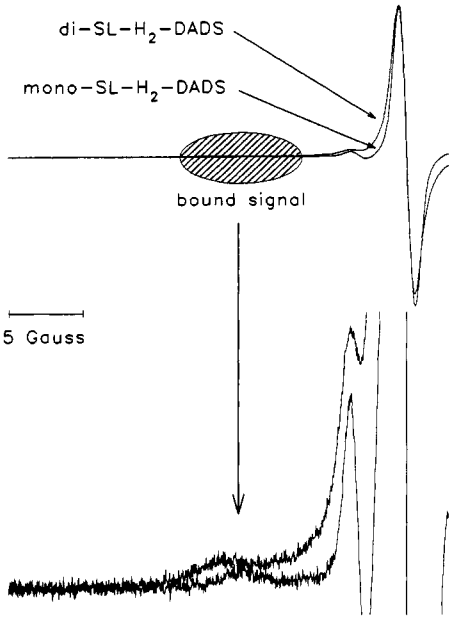

FIGURE 4: V_1 EPR spectra showing spin-label binding-induced low-field features in the EPR spectra of mono- and di-SL-H_2-DADS. In the top panel, the broad low-field bound peak is not discernible when compared with the peak height of the sharp unbound line. In the lower panel, the vertical scale has been expanded by a factor of 20 so that the immobilized features of the spectra from bound, immobilized probes can be seen.

of the solution, temperature-induced changes in viscosity are reflected in the line widths. Figure 3 shows the results of varying the temperature of a 100 μM aqueous sample of [^{14}N]-mono-SL-H_2-DADS (upper panel). As the sample temperature is increased, line widths sharpen as the viscosity decreases and rotational motion increases.

The EPR spectra from a 100 μM [^{14}N]di-SL-H_2-DADS sample recorded at 2, 22, and 40 °C (lower panel, Figure 3) show a result entirely different from that of the corresponding monoradical spectra. The temperature-induced changes in the diradical solution spectra are attributed to the spin relaxation effects of intramolecular exchange interactions. A higher temperature provides the energy necessary for interconversion to the energetically less favorable *cis* conformation, which brings the nitroxide moieties within approximately 8 Å, a distance which facilitates observation of spin–spin exchange (see Molecular Modeling Results). Although these line width effects are subtle, exchange coupling is clearly contributing to the solution spectra of the diradical spin-label. The importance of this observation for the current studies is that, under appropriate conditions, di-SL-H_2-DADS can apparently assume a compact, folded *cis* conformation where the two ends of the probe approach one another.

Equilibrium Binding of Mono- and Di-Spin-Labeled H_2-DADS. The EPR spectra recorded from samples of packed erythrocytes show concentration-dependent changes which confirm equilibrium binding of both mono- and di-spin-labeled H_2-DADS. Each V_1 EPR spectrum obtained from spin-label-containing erythrocyte suspensions is a composite spectrum which consists of a bound and an unbound component. Spin-label binding results in a relative reduction in the amplitude of spectral features attributable to the freely tumbling unbound spin-label. Likewise, there is also a relative increase in the amplitude of spectral features attributable to the immobilized bound spin-label. In the absence of cooperativity, the total concentration of spin-label in the sample is distributed between bound and unbound spin-label according to the simple chemical equilibrium relationship

$$[LR] \underset{k_a}{\overset{k_d}{\rightleftharpoons}} [L] + [R]$$

Certain features of EPR spectra are clearly distinguishable as representing bound and unbound spin-label. Figure 4 shows an expanded view of the low-field features of each spectrum which enable direct quantitation of spin-label binding. The line height of the *sharp* low-field line is proportional to the concentration of freely tumbling unbound spin-label, while the immobile bound spin-label results in a *broad* signal in the low-field region. The amount of bound spin-label in the sample can be determined by either measuring the height of the broad low-field bound signal or, because the total amount of spin-label in the sample must be constant, measuring the reduction in the height of the unbound sharp low-field line.

A standard curve, obtained by varying the concentration of free spin-label in a sample with no available binding sites, is required to quantitatively relate the changes in line height with known changes in spin-label concentration. The slope of the line fit through these data provides the conversion factor needed to relate peak heights to spin-label concentrations. Conversion factor data (not shown) were obtained by adding an appropriate aliquot of mono- or di-spin-labeled H_2-DADS to a sample of DIDS pretreated packed erythrocytes. DIDS pretreated packed cells were used instead of aqueous samples of spin-label in buffer to avoid errors due to the inherent differences in the dielectric properties between a sample of aqueous buffer and a sample of packed erythrocytes.

Binding data for both mono- and di-spin-labeled H_2-DADS are shown plotted in the upper panels of Figures 5 and 6. The data have been normalized by an estimate of the concentration of band 3 present in the sample. Band 3 protein concentrations are obtained by measuring the number of red blood cells per unit volume using a Coulter Counter and assuming the number of copies of the band 3 monomer per cell to be $\sim 1 \times 10^6$. Ideally, the binding curves should show saturation in binding at [bound]/[band 3] = 1.0 for a 1:1 binding stoichiometry. Slight deviations from unity can be explained by the variation in the number of copies of band 3 per cell which reportedly

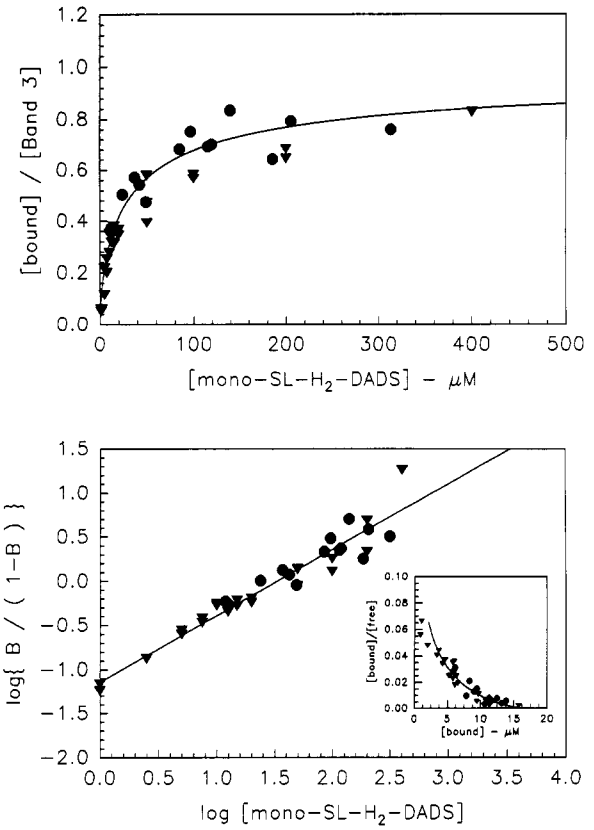

FIGURE 5: Binding data for mono-SL-H_2-DADS bound to intact erythrocytes (upper panel). The data (solid symbols) were obtained by two methods as described in the Experimental Procedures. The solid line shows the results of the best fit of all the data using the general binding equation discussed in the text. The best-fit constants were K_d = 11 μM and n = 0.67, which were obtained using nonlinear least-squares regression. In the lower panel of the figure are the corresponding Hill (slope 0.75 ± 0.02) and Scatchard plots (inset), illustrating the negative cooperativity in binding. Please see the Results for details. All data were collected at 20 °C.

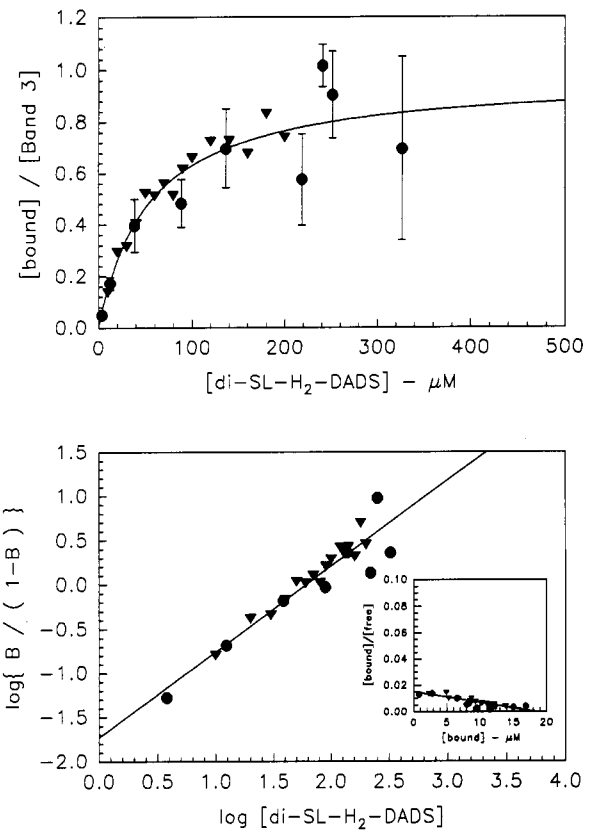

FIGURE 6: Binding data for di-SL-H_2-DADS bound to intact erythrocytes (upper panel). These data (solid symbols), as with the mono-spin-label, were obtained using two different experimental methods (see Experimental Procedures). The best-fit nonlinear regression curve (solid line) gives K_d = 54 μM and n = 0.98. In the lower panel of the figure are the corresponding Hill (slope 1.02 ± 0.02) and Scatchard plots (inset), illustrating no cooperativity (see Results). All data were collected at 20 °C.

varies among individuals from about 8×10^5 to 1.2×10^6 (Jennings, 1984).

Although the range of spin-label concentrations needed to provide complete binding curves should span several orders of magnitude, the practical range over which these measurements can be made is approximately 1–400 μM. Although this is less than ideal, this is a sufficient range to define the important binding properties. Data for the binding curves shown in Figures 5 and 6 were obtained, as described under Experimental Procedures, using two complementary methods which gave superimposable results.

For the first method (inverted triangles), the accurate determination of the peak height of the broad bound signal at very low spin-label concentrations is limited by the inherent signal-to-noise capabilities of the spectrometer. Likewise, at saturating concentrations of spin-label, obtaining the height of the bound peak is nearly impossible because of the subtraction artifacts introduced by the overwhelmingly large unbound signal generated by a huge excess of free spin-label.

The second method of measuring binding (circles) measures the reduction of unbound spin-label in the aqueous extracellular space due to binding. This method provides a means of measuring binding at higher concentrations where subtraction artifacts are most likely to obfuscate the bound spectrum, which is much more of a problem for the diradical spin-label than for the monoradical spin-label because of the spin-exchange-broadened lines. The binding data for di-SL-H_2-DADS at high concentrations obtained using this method are shown in Figure 6. These binding data, when taken alone or when combined with the data from the first method, yield the same values for binding constants and, either alone or combined, show no signs of cooperativity in the binding of di-SL-H_2-DADS, which is discussed below.

The binding data from both the mono- and the di-spin-label binding experiments were examined to determine if any cooperativity in spin-label binding is present. A general binding equation of the form

$$\frac{[\text{bound}]}{[\text{band 3}]} = \frac{a[\text{spin-label}]^n}{K_d + [\text{spin-label}]^n}$$

was fit to the binding data using a nonlinear least-squares method to determine the values of the parameters a, K_d, and n. The dissociation constants were found to be K_d = 11 μM for mono-SL-H_2-DADS and K_d = 54 μM for di-SL-H_2-DADS, indicating lower binding affinity for the larger disubstituted spin-label. The value of the exponent n signifies the absence of cooperativity when n = 1.0. A value for $n < 1.0$ indicates negative cooperativity is present, and correspondingly, positive cooperativity is present when $n > 1.0$. The exponent n is analogous to the slope of a Hill plot.

Nonlinear regression analysis of mono-SL-H_2-DADS binding data reveals that n = 0.67, indicating that significant negative cooperativity occurs in the binding of this stilbenedisulfonate to band 3. Linear regression of the mono-SL-H_2-DADS binding data replotted in the form of a Hill plot, shown in the lower panel of Figure 5, gives a slope of 0.75 ± 0.02, which is nearly the same value obtained by nonlinear

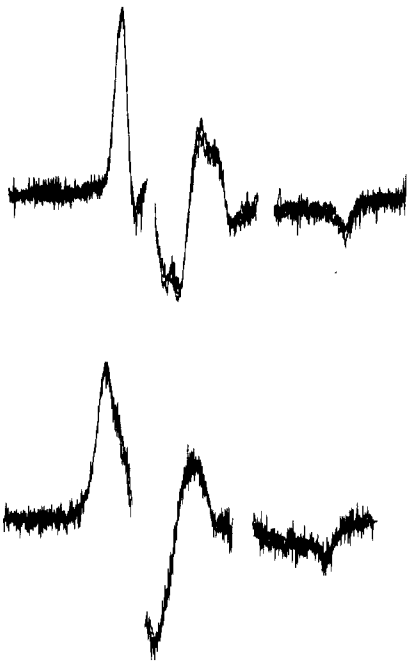

FIGURE 7: Bound spectra for [^{15}N]mono-SL-H_2-DADS obtained at spin-label concentrations of 4, 10, 20, 100, and 200 μM which are normalized and shown plotted on top of each other (upper panel). The small gaps in the spectra are due to artifacts introduced by the subtraction of the very large unbound signals. In the lower panel, [^{15}N]di-SL-H_2-DADS normalized bound spectra at 10, 30, and 100 μM are plotted. Each spectrum is 80 G in width and consists of 4096 data points. All spectra were collected at 20 °C.

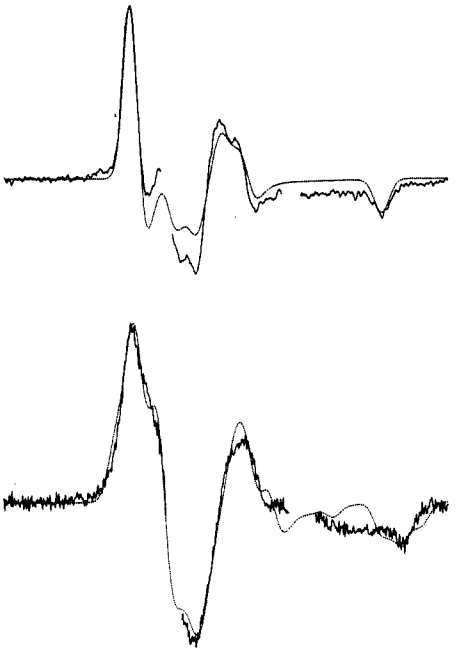

FIGURE 8: Experimental bound spectra shown together with the best-fit computed spectra. The best-fit mono-SL-H_2-DADS spectrum, shown in the upper panel, was obtained with the following parameter values: $g_x = 2.00862$, $g_y = 2.00571$, $g_z = 2.00217$, $A_x = 9.313$ G, $A_y = 8.959$ G, $A_z = 44.773$ G, and $T_2 = 2.1 \times 10^{-8}$ s. These values were used to find the values for the magnitude of the intramolecular interelectron vector, $|\mathbf{R}_{1,2}|$, and the angles ξ, η, A_1, A_2, and A_3 for bound di-SL-H_2-DADS. The following values were obtained: $|\mathbf{R}_{1,2}| = 17$ Å, $\xi = 65°$, $\eta = 23°$, $A_1 = 77°$, $A_2 = 80°$, and $A_3 = 13°$. The best-fit spectrum is shown in the lower panel.

regression analysis of the raw binding data. A Scatchard replot of the binding data is also shown in the lower panel of Figure 5 (inset). The nonlinear, downwardly concave Scatchard curve further illustrates the point that mono-SL-H_2-DADS binding to band 3 occurs with significant negative cooperativity. This curve intercepts the x axis at 17 μM, which is the same as the estimated concentration of band 3 monomers.

Nonlinear regression analysis of binding data for the larger di-SL-H_2-DADS probe reveals that $n = 0.98$, indicating that no cooperativity occurs in the binding of this compound. When the di-SL-H_2-DADS binding data are replotted in the form of a Hill plot (Figure 6, lower panel), the resulting slope is 1.02 ± 0.02. Likewise, the Scatchard plot, shown in the inset in the lower panel of Figure 6, is linear. Clearly, the disubstituted spin-label binds to band 3 with lower affinity and without any indication of negative cooperativity.

Electron–Electron Dipolar Interactions in Bound Spectra. The bound spectra, each obtained by digital subtraction of the free spin-label spectrum from the composite, were normalized to the broad low-field peak height and plotted in Figure 7. These spectra, obtained over a wide range of [^{15}N]-spin-label concentrations, overlie one another, thus demonstrating that no concentration-dependent alterations in line shape occur when either mono- or di-SL-H_2-DADS binds to the stilbenedisulfonate binding site of the band 3 protein. Any dipolar interactions between two adjacent immobilized spin-label molecules would result in line shape changes which would grow in dominance as saturating conditions were reached. Such changes, which are not seen in these data, would occur because the probability of the two neighboring binding sites on band 3 dimers both being occupied by spin-label molecules increases as available binding sites become saturated. The occupation of adjacent sites on a dimer is a nonlinear function of saturation. At low concentrations, there is a huge excess of binding sites, and most bound spin-label molecules will have the adjacent site unoccupied (in the absence of strong positive cooperativity in binding). At concentrations close to saturation, most dimers will have the two adjacent sites occupied.

The bound [^{15}N]mono-SL-H_2-DADS spectrum shown in Figure 8 (upper panel) was analyzed to determine the elements of the nitrogen hyperfine (**A**) and electron-Zeeman (**g**) tensors, as well as the line width, T_2. The inclusion of dipolar interaction or exchange terms was not required to obtain an excellent fit to the data. The bound [^{15}N]di-SL-H_2-DADS spectrum shown in Figure 8 (lower panel) is clearly different from the mono-spin-label spectrum. The low-field peak, in particular, is asymmetrically broadened, but not split, indicating that some weak dipolar interaction is present. The shape of the spectrum, however, does not change throughout the range of spin-label concentrations for which spectra could be obtained. Thus, the observed broadening can be attributed to intramolecular dipole–dipole effects when di-SL-H_2-DADS is bound to the stilbenedisulfonate binding site of band 3. The bound spectrum was analyzed to determine the distance and geometry parameters associated with the dipolar interactions seen between the two nitroxide moieties of the bound di-spin-label (Figure 8, lower panel). Dipolar analysis results show that di-SL-H_2-DADS binds to the stilbenedisulfonate binding site in a conformation which is partially folded from the completely *trans* conformation, so that the distance between unpaired electrons of the nitroxide groups is reduced from 23 Å (*all-trans*) to 17 Å.

Molecular Modeling Results. As discussed earlier, the EPR spectra from 100 μM aqueous samples of di-SL-H_2-DADS show the spin relaxation effects of intramolecular exchange interactions. A molecular model of the di-spin-label compound was constructed to determine if it was conformationally

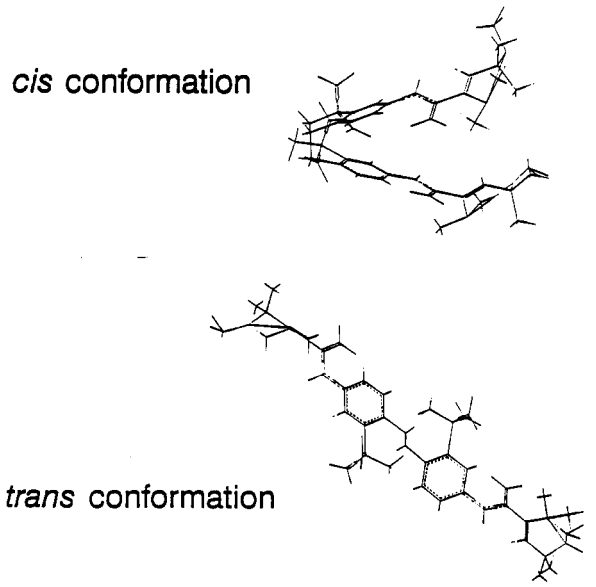

FIGURE 9: Predicted *cis* and *trans* conformations of di-SL-H_2-DADS, with the two nitroxide radicals separated by about 8 and 23 Å, respectively.

possible for the two nitroxide groups to be in close enough proximity to give rise to spin–spin coupling. The stick diagram shown in Figure 9 illustrates that an inter-nitroxide distance of about 8 Å occurs with the molecule in a *cis* conformation about the central methylene–methylene bond. In the *trans* conformation, the two nitroxide radicals are separated by about 23 Å. Molecular dynamics simulations (not shown) predict the *trans* conformation to be energetically favored over the *cis* conformation.

Verifying Specificity for the Anion Exchange Binding Site. Specificity of spin-label binding for the stilbenedisulfonate binding site of the band 3 protein was verified by looking for binding of these compounds following a saturating blockade of the binding sites by the specific irreversible anion exchange inhibitor DIDS. The EPR spectra shown in Figure 10 were recorded with and without pretreatment with 100 μM DIDS (see Experimental Procedures). The DIDS-pretreated spectra show the absence of the broad low-field peak, indicating that neither the mono- nor the di-spin-labeling reagent binds following blockage by DIDS.

DISCUSSION

Convincing evidence exists that dimeric band 3 is a stable complex in intact erythrocytes (Staros, 1982; Anjaneyulu et al., 1988; Nigg & Cherry, 1979; Jennings & Nicknish, 1985). However, the data needed to describe the monomer–monomer interface and the location of the stilbenedisulfonate binding site relative to this interface, and to each other, are sparse. The stoichiometry of binding of stilbenedisulfonate compounds to band 3 in intact erythrocytes is clearly one ligand molecule per band 3 monomer. The dimeric association between subunits is extremely tight, and isolated monomeric band 3 does not bind stilbenedisulfonates (Boodhoo & Reithmeier, 1984), which suggests that dimerization is a prerequisite for formation of the stilbenedisulfonate binding site and perhaps the anion exchange binding site as well. Thus, it is of interest to determine the spatial arrangement of the stilbenedisulfonate binding sites and to begin to understand to what extent and by what mechanisms these functionally important sites interact [reviewed in Salhany (1990)]. In the absence of high-resolution structural data, spectroscopic methods offer a reasonable opportunity for characterizing these sites.

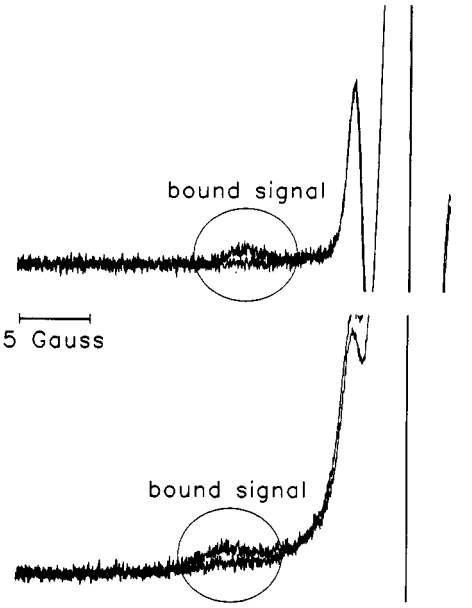

FIGURE 10: EPR spectra recorded using a high concentration (100 μM) of mono-SL-H_2-DADS both with and without pretreatment with a saturating concentration (100 μM) of the specific irreversible transport inhibitor DIDS (upper panel). DIDS pretreated cells give a flat line where the bound signal should be, indicating the absence of spin-label binding. The lower panel shows the same result when the same protocol was used with di-SL-H_2-DADS. Spectra were collected at 20 °C.

Transmembrane Disposition of the Stilbenedisulfonate Binding Site. Rao et al. (1979), using several fluorescent stilbenedisulfonate probes, have proposed that binding occurs in a rigid, hydrophobic cleft that extends deeply into the membrane. Macara et al. (1983) showed that eosin-5-maleimide, when reacted with the stilbenedisulfonate site on band 3, was quenched by the collisional quencher Cs^+ from the cytoplasmic surface of the membrane, suggesting that a conformational change accompanying or subsequent to binding leaves at least a portion of the eosin probe exposed to the intracellular side of the membrane. While the data collected in the present studies do not rule out the possibility that the central stilbene backbone might be exposed to the cell interior, they do provide evidence that the termini, containing the spin-label moieties, do not contact the cytosol. If the nitroxide moieties were in contact with the cell interior, the intracellular ascorbic acid would lead to rapid chemical reduction of the spin-label and concomitant loss of the EPR signal. No decrease in the EPR signal was observed in these studies unless extracellular ascorbate was added, which led to rapid loss of the signal (data not shown).

Steric versus Allosteric Interactions between Stilbenedisulfonate Binding Sites. Several researchers have reported that the reversible binding of some stilbenedisulfonate compounds shows negative cooperativity, which appears to depend on the size of the compound as well as on the buffer and experimental conditions employed. A large stilbenedisulfonate might sterically interfere with the binding of another large ligand to its neighboring subunit if the binding sites were spatially close together, but an intersubunit allosteric mechanism of cooperativity could also give the same result. Although mono-SL-H_2-DADS showed evidence of significant negative cooperativity, the larger di-SL-H_2-DADS molecule revealed no cooperativity in binding, which is not consistent with a steric mechanism. It would seem more likely that protein conformational changes, caused by the binding of a stilbenedisulfonate, perturb the monomer–monomer interface

so that the binding affinity on the adjacent subunit is altered. The characteristics of the molecular switch which determines cooperativity and the significance of cooperativity of ligand binding as related to the anion exchange function remain to be elucidated.

Distance Constraints Imposed by the Studies Presented. It is important to consider the inherent sensitivity of dipole–dipole interactions between nitroxide spin-labels for measurement of molecular distances. Like fluorescence resonance energy transfer experiments, the magnitude of spectral effects observed depends upon the relative orientation of the interacting probes. For X-band EPR, as used in the present studies, the maximum sensitivity to probe–probe separation would be observed if the nitroxide z axes (along the P_z orbital of the nitrogen of the N–O bond) were aligned with an axis extending between the two unpaired electrons (the interelectron axis). In this case, the extremum regions of the V_1 EPR spectrum would be split by $2\mathbf{D}$, where $\mathbf{D}$ is the unique element of the dipolar coupling tensor, and the interior turning points of the spectrum (x and y nitroxide axes) would be split by $\mathbf{D}$. With this geometry, clear splitting of extremum peaks can be seen with the high-resolution [^{15}N,^{2}H] probes at distances of 25 Å with observable line broadening to >27 Å. This represents the case of maximum sensitivity to a large distance. The minimum sensitivity to dipole–dipole coupling between nitroxides occurs when both nitroxide z axes are at the magic angle (54.7°) with respect to the interelectron axis. In this case, the extremum regions are not split at all by dipolar coupling regardless of the distance of closest approach. However, all other regions of the spectrum are still sensitive to the dipole–dipole interaction. Even with this unfavorable geometry, model calculations have shown that additional lines appear in the interior of the V_1 EPR spectrum at distances of 16 Å and that observable distortions of the spectrum can be seen out to near 20 Å with the narrow lines afforded by [^{15}N,^{2}H] probes.

Given these limits of sensitivity, it is instructive to consider the data presented in this work. With the mono-SL-H_2-DADS probe, the bound line shape is a classical powder pattern with all six turning points well-resolved at all concentrations of bound probe examined (Figures 7 and 8, upper panels). Additionally, the line width of the bound spectrum is comparable to immobilized, spatially isolated [^{15}N,^{2}H] spin-labels bound to other proteins (Beth et al., 1981; Anjaneyulu et al., 1988; Ajtai et al., 1992). At 200 μM mono-SL-H_2-DADS, 80% of the available band 3 binding sites were saturated (Figure 5). Thus, ~65% of the band 3 dimers had both binding sites occupied and should give rise to an EPR spectrum indicative of dipole–dipole coupling if the probes were within 20 Å regardless of the binding geometry. The data in Figure 7, upper panel, clearly show that no line shape alterations were observed at 200 μM probe concentration and that the 200 μM spectrum was indistinguishable from the 4 μM spectrum where very few dimers should have both sites occupied, especially given the negative cooperativity of binding observed with this probe.

Two potential complications must be considered before drawing absolute conclusions from the mono-SL-H_2-DADS data. First, the possibility exists of nonselective binding of this asymmetric probe within the stilbenedisulfonate site. With symmetric stilbenedisulfonates, it is unimportant which phenyl ring makes contact with which portion of the target binding site. However, with asymmetric probes, the possibility of random binding of the ring bearing the substituent to a specific region of the binding site could lead to decreased sensitivity,

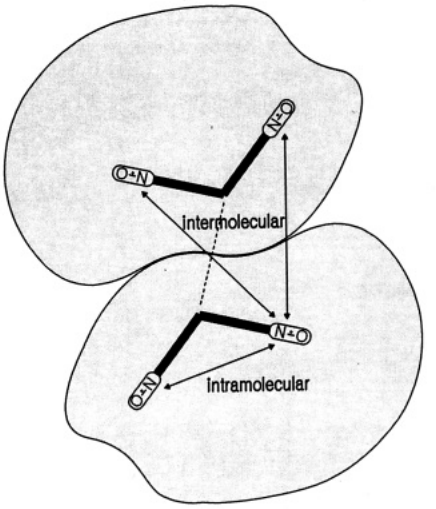

FIGURE 11: A schematic diagram depicting a model for dimeric band 3 which displays a 2-fold (C_2) axis of symmetry. Both outward-facing stilbenedisulfonate binding sites are shown occupied by the spin-label compound di-SL-H_2-DADS; the locations of the binding sites are arbitrarily shown. The arrows illustrate that information about the relative spatial arrangement between two intermolecular and one intramolecular nitroxide moieties of bound spin-label can potentially be obtained through electron–electron dipolar interactions when the internitroxide distances are within about 20 Å.

but not total loss of sensitivity, to observation of probe–probe interactions. Second, the possibility exists that ends of the stilbenedisulfonate sites on adjacent monomers are spatially close together but that opposite ends are far apart. If binding energies directed the spin-label moieties of mono-SL-H_2-DADS to opposite ends, then sensitivity to the distance of closest approach would be lost.

It was these potential complications which prompted the synthesis of di-SL-H_2-DADS. As a reporter molecule to study band 3, this compound is unique because it contains two point reporter groups on opposite ends of a long conformationally flexible molecule. This probe has the potential to report 3 times the spatial information of the monosubstituted probe without the complications previously discussed for the asymmetric mono-SL-H_2-DADS probe. Figure 11 depicts the one intramolecular and two intermolecular distances which potentially can be measured.

Conformation of Stilbenedisulfonates When Bound to Band 3. The data presented in Figure 7, lower panel, clearly show that, at all probe concentrations examined with di-SL-H_2-DADS, the EPR spectrum was broadened and major peaks were shifted relative to the corresponding spectrum obtained with mono-SL-H_2-DADS (Figure 7, upper panel). Two points about the EPR data from di-SL-H_2-DADS must be made. First, the distorted line shape (i.e., distorted from a spatially isolated nitroxide powder pattern) was observed at 10 μM probe concentration. Even in the absence of negative cooperativity in binding, probability considerations dictate that the majority of bound probes at this low concentration will be in a stilbenedisulfonate site without the corresponding site on the adjacent monomer of the dimer occupied. Thus, the distorted line shape at low concentrations was assigned to dipole–dipole coupling between the two spin-labels on the same di-SL-H_2-DADS probe (intramolecular dipole–dipole coupling, Figure 11). Second, the line shapes obtained at all higher concentrations were identical to the one obtained at 10 μM (Figure 7, lower overlays). At 100 μM and higher concentrations, a significant number of band 3 dimers would have both their stilbenedisulfonate sites occupied by di-SL-H_2-DADS. The complete absence of additional spectral

broadening and/or shifting of resonance lines at the highest concentrations examined supports the conclusion that both intermolecular distances depicted in Figure 11 are greater than 20 Å.

Assignment of the spectrum obtained with di-SL-H_2-DADS to dipole–dipole coupling between the two spin-label moieties versus other potential mechanisms of spectral distortion (e.g., vastly different mobilities of the two spin-label moieties of di-SL-H_2-DADS when bound to band 3 or spin–spin exchange interactions between the two spin-label moieties) is supported by the computer modeling results shown in Figure 8, lower panel. A reasonable fit of the bound spectrum was obtained using the **A** and **g** tensors and T_2 from fitting the mono-SL-H_2-DADS (Figure 8, upper panel) and varying $|\mathbf{R}_{1,2}|$, ξ, η, A_1, A_2, and A_3 as described in the Experimental Procedures. Given the number of degrees of freedom required for fitting the experimental data, the agreement between experimental and calculated data is reasonable. While several combinations of the orientational variables (ξ, η, A_1, A_2, and A_3) gave similar χ^2 values, each of these combinations was grouped around an interelectron separation, $|\mathbf{R}_{1,2}|$, of 17 Å. If one assumes a single bend in di-SL-H_2-DADS centered at the ethyl bridge between the two phenyl rings, a 17-Å distance between nitroxide moieties predicts a bend angle of approximately 100°. These values for $|\mathbf{R}_{1,2}|$ and the overall bend are entirely consistent with molecular models for di-SL-H_2-DADS (Figure 9). In the completely extended conformation, molecular models predict an $|\mathbf{R}_{1,2}|$ of 23 Å and a bend angle of approximately 180°. In the folded, or *cis*, conformation, $|\mathbf{R}_{1,2}|$ can decrease to 8 Å and the bend angle to approximately 40°. The experimental values determined for the probe when bound to band 3 are between these two extremes.

Comparison of Distance Constraints with Previous Studies. Determination of a bend angle of 100° permits some speculation on the limits of closest approach of portions of the di-SL-H_2-DADS molecules within the constraints of intermolecular separations between the ends of the bound probes. Using the planar model depicted in Figure 11, it is possible that the central ethyl bridges of adjacent probes can approach within 5 Å of each other (dashed line in Figure 11) without the ends approaching closer than 20 Å. This simplified model demonstrates that, on the basis of the data obtained in the present work alone, reasonably close approach of the central portions of adjacent probes cannot be ruled out. However, when the present data are combined with previous studies using other probes (Anjaneyulu et al., 1988; Macara & Cantley, 1981), it appears likely that the stilbenedisulfonate sites are lengthwise reasonably well separated. Results obtained from these present studies reasonably complement the previous energy transfer studies of Macara & Cantley (1981) by setting a minimal separation between specific loci of the stilbenedisulfonate probes bound to band 3. While the exact number of membrane-spanning segments have not been determined with certainty, hydropathy considerations and various labeling data have led to working models for the linear arrangement of the membrane-spanning segments of band 3 [reviewed in Jennings (1989)]. Estimates range between 10 and 16 such segments, and the α-helical content of these membrane-spanning domains is high (Oikawa et al., 1985). Assuming a model of 10 membrane-spanning α-helices for the band 3 monomer, a lower limit based upon current data, a separation of 20 Å between stilbenedisulfonate binding sites is certainly consistent with the predicted overall dimension of a band 3 dimer in the plane of the membrane.

In conclusion, the present studies have provided support for an allosteric coupling between stilbenedisulfonate binding sites on band 3 in intact erythrocytes. Data from both mono- and di-SL-H_2-DADS probes have indicated a minimum of 20-Å separation between the termini of the stilbenedisulfonate binding sites on adjacent monomers of the membrane oligomer. Finally, studies with di-SL-H_2-DADS have allowed definition of the expanse of the stilbenedisulfonate site in terms of the degree of bending induced upon the bound probe.

ACKNOWLEDGMENT

We thank Dr. Eric Hustedt for assistance in fitting EPR data and Drs. Charles Cobb and Wayne Anderson for helpful discussion about the paper. We also thank Drs. Wayne Anderson and Marcia Newcomer for assistance with the molecular modeling portion of this work. The Mass Spectroscopy Center at Vanderbilt University provided valuable assistance in obtaining mass spectral data for the compounds synthesized in this work.

REFERENCES

Ajtai, K., Ringler, A., & Burghardt, T. P. (1992) *Biochemistry 31*, 207–217.
Anjaneyulu, P. S. R., Beth, A. H., Sweetman, B. J., Faulkner, L. A., & Staros, J. V. (1988) *Biochemistry 27*, 6844–6851.
Barzilay, M. & Cabantchik, Z. I. (1979) *Membr. Biochem. 2*, 255–267.
Beth, A. H., Venkataramu, S. D., Balasubramanian, K., Dalton, L. R., Robinson, B. H., Pearson, D. E., Park, C., & Park, J. H. (1981) *Proc. Natl. Acad. Sci. U.S.A. 78*, 967–971.
Beth, A. H., Robinson, B. H., Cobb, C. E., Dalton, L. R., Trommer, W. E., Birktoft, J. J., & Park, J. H. (1984) *J. Biol. Chem. 259*, 9717–9728.
Boodhoo, A. & Reithmeier, R. A. F. (1984) *J. Biol. Chem. 259*, 785–790.
Cabantchik, Z. I. & Rothstein, A. (1972) *J. Membr. Biol. 10*, 311–330.
Cabantchik, Z. I. & Rothstein, A. (1974) *J. Membr. Biol. 15*, 207–226.
Casey, J. R. & Reithmeier, R. A. F. (1991) *J. Biol. Chem. 266*, 15726–15737.
Cobb, C. E., Juliao, S., Balasubramanian, K., Staros, J. V., & Beth, A. H. (1990) *Biochemistry 29*, 10799–10806.
Dix, J. A., Verkman, A. S., & Solomon, A. K. (1986) *J. Membr. Biol. 89*, 211–223.
Eaton, S. S., More, K. M., Sawant, B. M., Boymel, P. M., & Eaton, G. R. (1983) *J. Magn. Reson. 52*, 435–449.
Hustedt, E. J., Cobb, C. E., Beth, A. H., & Beechem, J. M. (1993) *Biophys. J. 64*, 614–621.
Jay, D. & Cantley, L. (1986) *Annu. Rev. Biochem. 55*, 511–538.
Jennings, M. L. (1984) *J. Membr. Biol. 80*, 105–117.
Jennings, M. L. (1989) *Annu. Rev. Biophys. Biophys. Chem. 18*, 397–430.
Jennings, M. L. & Nicknish, J. S. (1985) *J. Biol. Chem. 260*, 5472–5479.
Knauf, P. A. (1979) *Curr. Top. Membr. Transp. 12*, 249–363.
Lepke, S., Fasold, H., Pring, M., & Passow, H. (1976) *J. Membr. Biol. 29*, 147–177.
Macara, I. G. & Cantley, L. C. (1981) *Biochemistry 20*, 5095–5105.
Macara, I. G., Kuo, S., & Cantley, L. C. (1983) *J. Biol. Chem. 258*, 1785–1792.
Margaritis, L. H., Elgsaeter, A., & Branton, D. (1977) *J. Cell Biol. 72*, 47.
Nigg, E. A. & Cherry, R. J. (1979) *Biochemistry 18*, 357–365.
Oikawa, K., Lieberman, D. M., Reithmeier, R. A. F. (1985) *Biochemistry 24*, 2843–2848.
Passow, H. (1986) *Rev. Physiol. Biochem. Pharmacol. 103*, 61–203.
Press, W. H., Flannery, B. P., Teukolsky, S. A., & Vetterling,

W. T. (1989) *Numerical Recipes (FORTRAN Version)*, pp 289–293, Cambridge University Press, New York.
Rao, A., Martin, P., Reithmeier, R. A. F., & Cantley, L. C. (1979) *Biochemistry 18*, 4505–4516.
Rozantsev, E. G. (1970) *Free Nitroxyl Radicals*, pp 209–210, Plenum Press, New York.
Salhany, J. M. (1990) *Erythrocyte Band 3 Protein*, pp 1–213, CRC Press, Boca Raton, FL.
Salhany, J. M. & Sloan, R. L. (1988) *Biochem. Biophys. Res. Commun. 156*, 1215–1222.
Ship, S., Shami, Y., Breuer, W., & Rothstein, A. (1977) *J. Membr. Biol. 33*, 311–324.
Staros, J. V. (1982) *Biochemistry 21*, 3950–3955.
Staros, J. V. & Kakkad, B. P. (1983) *J. Membr. Biol. 74*, 247–254.
Steck, T. L. (1972) *J. Mol. Biol. 66*, 295–305.
Verkman, A. S., Dix, J. A., & Solomon, A. K. (1983) *J. Gen. Physiol. 81*, 421–449.
Weinstein, R. S., Khodadad, J. K., & Steck, T. L. (1980a) in *Membrane Transport in Erythrocytes* (Lassen, U. V., Ussing, H. H., & Wieth, J. O., Eds.) pp 35–46, Munksgaard, Copenhagen.
Weinstein, R. S., Khodadad, J. K., & Steck, T. L. (1980b) *J. Cell Biol. 87*, 209.
Wojcicki, W. E., Cobb, C. E., & Beth, A. H. (1992) *Biophys. J. 61*, A522.